Carbohydrate Polymers 87 (2012) 2546–2553

Contents lists available at SciVerse ScienceDirect

Carbohydrate Polymers

journal homepage: www.elsevier.com/locate/carbpol

# Cellulose isolation and core–shell nanostructures of cellulose nanocrystals from chardonnay grape skins

Ping Lu, You-Lo Hsieh*

*Fiber and Polymer Science, University of California, Davis, CA 95616, USA*

ARTICLE INFO

*Article history:*
Received 7 October 2011
Received in revised form 8 November 2011
Accepted 8 November 2011
Available online 17 November 2011

*Keywords:*
Chardonnay grape skins
Cellulose nanocrystals
Nanoparticles
Nano-rods
Core–shell self-assembly

ABSTRACT

This is the first report on the derivation and structures of cellulose nanocrystals from grape skins. Pure cellulose was isolated from chardonnay grape skins at a 16.4% yield by a process involving organic extraction, acid and base dissolutions, and basic and acidic oxidation. The as-extracted cellulose was 54.9% crystalline and microfibrillar. Acid hydrolysis (64–65% $H_2SO_4$ 45 °C, 30 min) of grape skin cellulose produced the more crystalline (64.3%) cellulose nanocrystals (CNCs) that appeared mostly as spherical nanoparticles with diameters ranging from 10 to 100 nm and a mean diameter of 48.1 (±14.6) nm as observed by TEM. AFM further disclosed the spherical nanoparticles actually consist of a nano-rod core (seed) surrounded by numerous tiny cellulose fragments as the shell. Interestingly, the spherical core–shell nanoparticles resemble the shape of grape bundles, the starting biomass, may be assembled via interfacial hydrogen bonds.



## 1. Introduction

Grape is the world's largest fruit crop, with around 7.6 million ha dedicated to vineyards and an estimated 67 million tons annual production worldwide (FAOSTAT, 2009). Approximately 80% of the grape produced is used in winemaking with a smaller portion going to juice production. France, Spain, Italy and United States are the major grape producers and where wine industry constitutes an important part of the economy and culture (Meyer, Pinelo, & Arnous, 2006). Beverage processing of grapes leaves behind a huge amount of pressed residue or "pomace" as the by-product, which is estimated to be at least 50 million tons per annum (Meyer & Arnous, 2008). These grape beverage wastes are currently disposed by composting, incineration, as landfills or for other agronomic applications (Spigno, Pizzorno, & De Faveri, 2008). Although the grape pomace is not intrinsically hazardous, the concentrated disposal in a particular time period of the year and the release of high levels of organics such as phenolics, pose potential environmental concerns (Brosse, Ping, Sannigrahi, & Ragauskas, 2011; Spigno et al., 2008). Grape pomace has also been shown to inhibit germination by immobilizing plant nutrients (Cambardella, Richard, & Russell, 2003; Vazquez, Moldes, Dominguez, Diaz-Fierros, & Barral, 2007, 2008) in addition to increasing the biological and chemical oxygen demands (Spigno & De Faveri, 2007). Rational and sustainable utilization of grape pomace to develop new bioproducts would be of great benefit to not only diminish adverse environmental impact but also create new value-added avenue.

Grape pomace includes stalks, skins, pulps and seeds (Gomez-Brandon, Lazcano, Lores, & Dominguez, 2011) and consists of mainly cellulose, lignin, hemicellulose and other polysaccharides (Gomez-Plaza, Ortega-Regules, Romero-Cascales, Ros-Garcia, & Lopez-Roca, 2006; Lorenzo, Moldes, Couto, & Sanroman, 2002; Nunan, Sims, Bacic, Robinson, & Fincher, 1997; Paradelo, Moldes, & Barral, 2010). In contrast to other lignocellulosic biomasses (e.g., wood, straw, etc.), however, skins of grape pomace contain unique phenolic compounds (Souquet, Labarbe, Le Guerneve, Cheynier, & Moutounet, 2000) that have received tremendous attention for their potential application as food antioxidants (Amendola, De Faveri, & Spigno, 2010; Meyer et al., 2006; Pinelo, Rubilar, Jerez, Sineiro, & Nunez, 2005; Spigno & De Faveri, 2007). Extraction of the phenolics from grape skins still leaves significant quantity of grape lignocellulosic residues, potential sources for deriving other value added products.

This study is the first to isolate pure cellulose from grape skins generated from white winemaking process and to derive cellulose nanocrystals. Several chemical processes reported for biomass separation including solvent extraction, acid/base dissolution and oxidation/reduction over a wide range of reaction conditions (Abe & Yano, 2009; Alemdar & Sain, 2008; Nogi, Iwamoto, Nakagaito, & Yano, 2009; Sun, Sun, Zhao, & Sun, 2004; Sun, Tomkinson, Mao, & Sun, 2001) have been evaluated to design the most effective approach to isolate cellulose from grape skins collected from chardonnay winemaking process. The primary objective was to effectively isolate cellulose by removing all non-cellulosic

* Corresponding author. Tel.: +1 530 752 0843; fax: +1 530 752 7584.
*E-mail address:* ylhsieh@ucdavis.edu (Y.-L. Hsieh).

0144-8617/$ – see front matter © 2011 Elsevier Ltd. All rights reserved.
doi:10.1016/j.carbpol.2011.11.023

compositions such as pectin, phenolics, lignin and hemicellulose with organic solvent extraction, acid and base dissolution as well as peroxide oxidation under mild conditions. The second goal was to prepare cellulose nanocrystals from grape skin cellulose by acid hydrolysis reported for wood (Dong & Roman, 2007), cotton (Lu & Hsieh, 2010) and rice (Lu & Hsieh, 2011) cellulose.

## 2. Experimental

### 2.1. Materials

Grape skins from chardonnay grape in the winemaking process (SonomaCeuticals, Santa Rosa, CA) were used in this study. The skins were separated from other solids by passing the chardonnay pomace over a shaker table equipped with varied grating sizes to remove the seeds and stems, leaving the skins. Toluene (99.5%, ACS GR, Sigma–Aldrich), ethanol (anhydrous, EMD), sulfuric acid (95–98%, ACS GR, EMD), sodium hydroxide (>97%, ACS GR, EMD), hydrogen peroxide (30%, ACS GR, EMD), sodium chlorite (80%, Fluka) and acetic acid glacial (99.7%, ACS GR, EMD) were used as received without further purification. All water used was purified by Milli-Q plus water purification system (Millipore Corporate, Billerica, MA).

### 2.2. Isolation of cellulose from grape skins

The non-cellulosic components in grape skins were removed to isolate cellulose by incorporating and streamlining procedures reported for varied biomass sources (Abe & Yano, 2009; Alemdar & Sain, 2008; Nogi et al., 2009; Sun et al., 2001, 2004). The as-received grape skins was milled (Thomas-Wiley Laboratory Mill model 4, Thomas Scientific, USA) to pass through a 60-mesh screen, followed by oven-drying at 70 °C for 2 days. The dry grape skin powders (30 g) were first extracted with 2:1 v/v toluene/ethanol (450 mL) mixture for 20 h to remove wax, phenolics, pigments and oils, followed by oven-drying at 70 °C for 24 h. The organic-extracted powders were then heated in 2% $H_2SO_4$ (600 mL) aqueous solution under constant stirring at 90 °C for 5 h to hydrolyze acid soluble polysaccharides and polyphenolics, filtered and washed with water to neutral pH. The acid treated powders were further leached with 5% NaOH (600 mL) at the ambient temperature for 24 h and continued at 90 °C for 5 h to dissolve hemicellulose and other base soluble polysaccharides, filtered and thoroughly washed to neutral pH. The base treated sample was bleached by 5% $H_2O_2$ (600 mL) with pH adjusted to 11.5 by NaOH at 45 °C for 8 h (more $H_2O_2$ as well as higher temperature, e.g., 70 °C, may be necessary according to the sample color change), then cooled to ambient temperature for 24 h to oxide and dissolve lignin and phenolics. The bleaching effect was enhanced by continuing the reaction in 1.4% acidified $NaClO_2$ (1000 mL), with pH adjusted to 3.0–4.0 by $CH_3COOH$, at 70 °C for 5 h then at ambient temperature for 24 h to dissolve all the residual lignin, phenolics and other impurities. The final product was washed with water until neutral. The aqueous suspension (~300 mL) was quickly frozen by pouring liquid nitrogen ($N_2$) into the sample container and freeze-dried (FreeZone 1.0 L Benchtop Freeze Dry System, Labconco, Kansas City, MO) to remove water.

### 2.3. Preparation of nanostructures from grape cellulose

Cellulose isolated from grape skins was hydrolyzed using 64–65 wt% sulfuric acid at an 8.75 mL/g acid-to-cellulose ratio as previously reported for wood pulp (Dong & Roman, 2007) and cotton (Lu & Hsieh, 2010), and at a temperature of 45 °C for 30 min. Acid hydrolysis was stopped by diluting with 10-fold ice water. The resulting cellulose gel was washed once, centrifuged at 5000 rpm for 25 min at 10 °C, and then dialyzed using regenerated cellulose dialysis membranes with 12–14 kDa molecular weight cut off (Fisherbrand, Pittsburgh, PA) against ultra-pure water (Millipore Milli-Q UF Plus) until reaching neutral pH. The suspension was sonicated (Branson ultrasonic processor model 2510, Danbury, CT) in an ice bath for 30 min, and then filtered (Whatman 541, Maidstone, Kent, England) to remove larger pieces of aggregates. The suspension of cellulose nanocrystals (CNCs) at about 0.01 wt% was quickly frozen by pouring liquid nitrogen into the sample container and freeze-dried overnight to remove water. The dried product was stored under vacuum for the following characterizations.

### 2.4. Characterization

#### 2.4.1. Fourier transform infrared spectroscopy (FTIR)

FTIR spectra were collected using a Thermo Nicolet 6700 spectrometer (Thermo Fisher Scientific, USA). Samples were grounded with KBr (1:100, w/w) and pressed into transparent disks. The spectra were measured in the transmittance mode from an accumulation of 128 scans at a 4 $cm^{-1}$ resolution over 4000–400 $cm^{-1}$ range.

#### 2.4.2. Differential scanning calorimetry (DSC)

DSC measurements were carried out with DSC-60 differential scanning calorimeter (Shimadzu, Japan). The data were collected by heating approximate 5 mg sample in a sealed aluminum pan at a ramping rate of 10 °C/min from 30 to 600 °C under $N_2$ atmosphere with a flow rate of 30 mL/min.

#### 2.4.3. Thermogravimetric analysis (TGA)

TGA analyses were performed on TGA-50 thermogravimetric analyzer (Shimadzu, Japan). In a typical experiment, samples with a weight of around 10–20 mg were placed in a clean platinum pan and the data were recorded by heating the samples at 10 °C/min from ambient temperature (around 30 °C) to 600 °C in $N_2$ with a purging rate of 50 mL/min.

#### 2.4.4. Wide-angle X-ray diffraction (XRD)

The overall crystalline phases of samples were determined by XRD measurement on a Scintag XDS 2000 powder diffractometer. XRD samples were prepared by pressing the powders between two glass slides into a flattened sheet. Radial scans of intensity were recorded over scattering $2\theta$ angles from 5 to 40° (step size = 0.02°, scanning rate = 2 s/step) using a Ni-filtered Cu Kα radiation (λ = 1.5406 Å), an operating voltage of 45 kV, and a filament current of 40 mA. Crystallinity index (CrI) of each sample was calculated by referring to diffraction intensity of crystalline and amorphous regions using the following empirical equation (Segal, Creely, Martin, & Conrad, 1959) (1):

$$\mathrm{CrI} = \frac{(I_{2\,0\,0} - I_{\mathrm{am}})}{I_{2\,0\,0}} \times 100 \quad (1)$$

where $I_{2\,0\,0}$ is the peak intensity at plane (2 0 0) ($2\theta$ = 22.7°), and $I_{\mathrm{am}}$ is the minimum intensity at the valley between plane (2 0 0) and (1 1 0) ($2\theta$ = 18.7°).

#### 2.4.5. Scanning electron microscopy (SEM)

The microstructures and surface morphologies were examined by a field emission scanning electron microscope (FE-SEM) (XL 30-SFEG, FEI/Philips, USA). The samples were mounted on aluminum stubs with conductive carbon tapes and sputtered with gold under vacuum at 20 mA for 2 min (Bio-Rad SEM coating system). The samples were observed and imaged at a 5-mm working distance and a 10-kV accelerating voltage.

*2.4.6. Transmission electron microscopy (TEM)*

For TEM observation, a drop of 10 μL diluted CNC suspension (0.001, w/w%) after dialysis and filtration was deposited onto glow-discharged carbon-coated TEM grids (300-mesh copper, formvar-carbon, Ted Pella Inc., Redding, CA) and the excess liquid was removed by blotting with a filter paper after 2 min. The specimens were then negatively stained with 2% uranyl acetate solution for 2 min, blotted with a filter paper to remove excess stain solution and allowed to dry at ambient condition. The samples were observed using a Philip CM12 transmission electron microscope operated at a 100 kV accelerating voltage. The dimensions of CNCs were measured on 169 representative CNCs using analySIS FIVE and the size distribution analyzed by Origin Pro.

*2.4.7. Atomic force microscopy (AFM)*

AFM imaging of CNCs was performed with an Asylum Research MFP-3D atomic force microscope (Santa Barbara, CA). A few drops of the diluted suspension (0.001, w/w%) were deposited onto a freshly cleaved mica surface (Highest Grade V1 Mica Discs, 15 mm, Ted Pella, Inc.) and allowed to dry. Samples were scanned at ambient relative humidity and temperature in tapping mode with OMCL-AC160TS standard silicon probes (tip radius < 10 nm, spring constant = 28.98 N/m, resonant frequency = ~310 kHz) (Olympus Corp.) under a 1 Hz scan rate and an image resolution of 512 × 512 pixels. Image processing was performed with Igor Pro 6.21 loaded with MFP3D 090909+1409 modulus. The diameters and heights were determined from AFM height images.

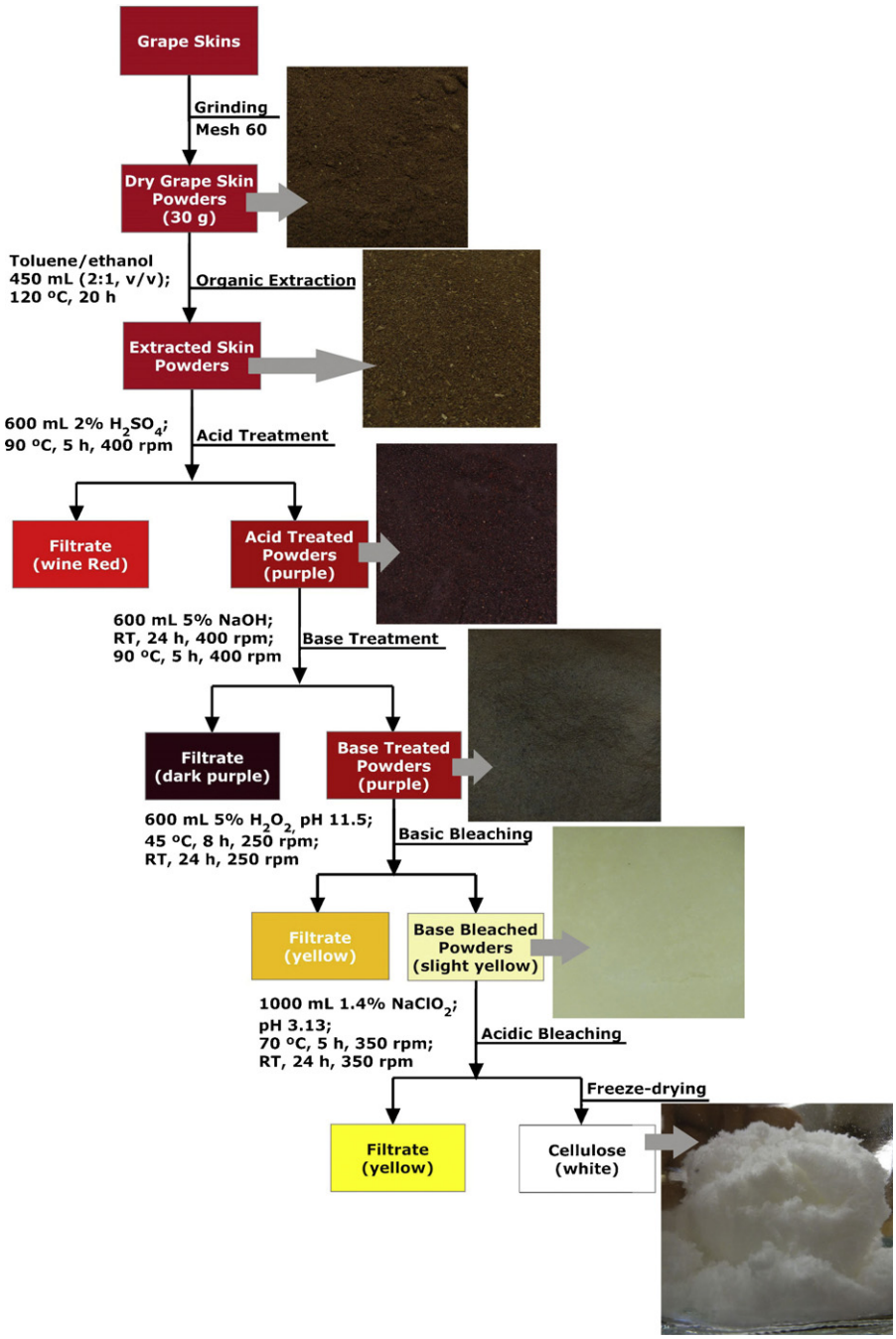


**Fig. 1.** Scheme of the experimental procedures for isolating cellulose from grape skins and the photographic images of corresponding solids at each step.

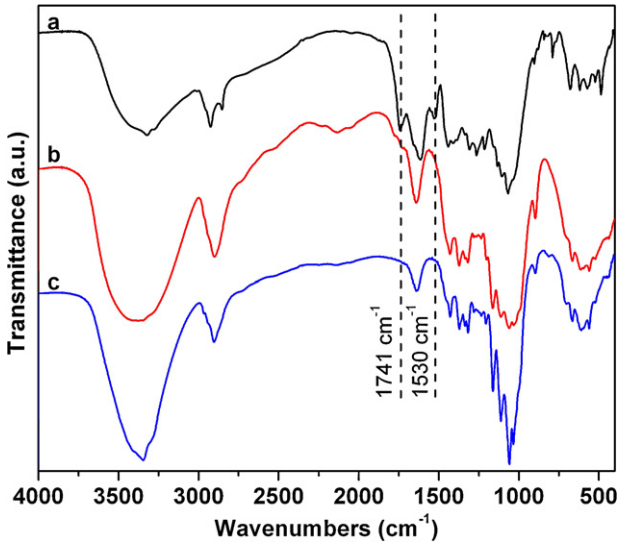


**Fig. 2.** FTIR of (a) grape skins, (b) as-extracted cellulose and (c) cellulose nanocrystals.

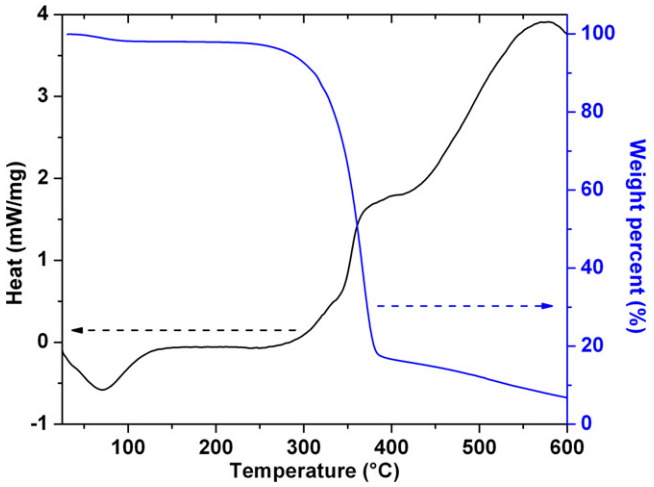


**Fig. 3.** Thermal properties of as-extracted cellulose from grape skins (black: DSC; blue: TGA). (For interpretation of the references to color in this figure legend, the reader is referred to the web version of the article.)

## 3. Results and discussion

### 3.1. Isolation of cellulose from grape skins

Cellulose was successfully extracted from chardonnay grape skins through a straightforward five-step process that includes organic extraction, acid and base treatments, basic and acidic oxidation and bleaching (Fig. 1). The organic extraction with a 2:1 (v/v) toluene/ethanol mixture was aimed to remove wax, oil, organic-soluble phenolics and other organic solubles. The originally clear mixture turned brownish-yellow after the extraction, showing dissolution of some colored substances. This organic extract also reduced the dark brown color of the grape skins to a lighter brown when dried, consistent with the removal of some organic soluble color substances. The following acid treatment turned the brown color of the powders to purple and produced a filtrate with a beautifully vivid wine red color. The 2% $H_2SO_4$ treatment (90 °C, 5 h) was designed to dissolve phenolic acids and remove polysaccharides such as pectin and xylan by hydrolyzing them into sugars. The color changes corresponded to the removals of acid-soluble, colored phenolics and the corresponding compositional change. The base treatment (5% NaOH, 24 h) was to dissolve hemicellulose and some polyphenolics such as tannins. The basic filtrate was indeed a very dark purple. However, the powders still appeared purple-brown. The most significant color changes of both the powders and filtrate were observed after the basic oxidation and bleaching process ($H_2O_2$, pH 11.5, 45 °C, 8 h). The powders turned mostly white with a faint light yellow, indicating the successful removal of most colored compositions such as lignin and phenolics. The oxidation and bleaching effect were further enhanced by acidic bleaching ($NaClO_2$, pH 3–4, 70 °C, 5 h). Pure white product was derived after the five-step process with a total yield of 16.4% from the chardonnay grape skins.

The FTIR spectra of the resultant white product confirmed its chemical structure to be cellulose (Fig. 2). The spectrum of grape skins shows abundant sharp absorption peaks in the 1500–500 $cm^{-1}$ fingerprint region (Fig. 2a), disclosing the tens, if not hundreds, of the complex compositions in the grape skins reported (Meyer & Arnous, 2008; Meyer et al., 2006; Souquet et al., 2000). The most distinct spectral change in the white product is the absence of two peaks at 1741 (carbonyl stretching) and 1530 (aromatic skeletal vibrations) $cm^{-1}$ (Fig. 2b). The 1741 $cm^{-1}$ carbonyl peak indicates the presence of polysaccharides, such as pectin, xylan and hemicellulose, as well as some phenolic acids. The peak at 1530 $cm^{-1}$ comes from the aromatic structures that are typical of the phenolics. The absence of these two peaks from the spectrum of the white product confirms the complete removal of other polysaccharides and phenolics in grape skins. Most significantly, FTIR of the white product (Fig. 2b) clearly showed all the characteristic absorptions of cellulose, including the broad bands in the 3650–3000 $cm^{-1}$ region assigned to O–H stretching vibration, the peak at 2900 $cm^{-1}$ corresponding to C–H stretching vibration, absorption at 1430 $cm^{-1}$ designated to the bending of –C-6–$CH_2$– and the deformation, wagging, and twisting modes of the anhydroglucopyranose units in the 1800–600 $cm^{-1}$ region (Lu & Hsieh, 2010, 2011).

The thermal profiles of the white product measured by DSC and TGA, shown in Fig. 3, also match perfectly to that of cellulose. The initial DSC endothermic peak between 30 and 130 °C is due to the evaporation of absorbed moisture, and corresponds to a 1.9% mass loss in TGA data. The 130–260 °C region in the DSC was leveled, showing only 1.2% mass loss in the TGA, also characteristic of cellulose. Significant thermal degradation was observed as broad DSC exotherms beginning at 280 °C and up to 570 °C. A significant weight loss of 79.0% was observed between 260 and 385 °C in the TGA, which is a typical decomposition characteristic of cellulose. The total weight loss is calculated to be 93.2%, close to our previously reported value for cotton cellulose (Lu & Hsieh, 2010).

XRD diagram of the product shows four diffraction peaks at $2\theta = 14.7$, 16.4, 22.7 and 34.6° (Fig. 4a), characteristic of cellulose crystal assignments of the $1\bar{1}0$, 110, 200 and 004 planes, respectively (Wada, Heux, & Sugiyama, 2004). The crystallinity index (CrI) was calculated to be 54.9% using the empirical Segal equation (Segal et al., 1959). This CrI value is lower than cellulose isolated from wood (73.5%) (Renneckar & Li, 2011), cotton (65.0%) (Lu & Hsieh, 2010) and rice (61.8%) (Lu & Hsieh, 2011) cellulose. The XRD crystalline structural data, together with FTIR chemical structural compositions and DSC and TGA thermal behaviors, confirmed the isolated white product to be pure cellulose. These structural analyses demonstrated the step-wise process of organic/acid/base/oxidation to be highly effective in isolating cellulose from grape skins. This successful approach to isolate cellulose from white grape skins serves as an excellent prototype for extract cellulose from other phenolic-rich biomass.

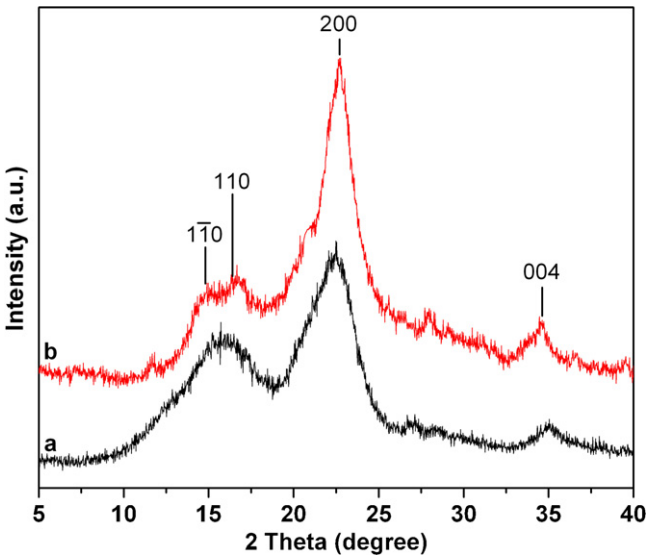


**Fig. 4.** XRD of (a) as-extracted cellulose from grape skins and (b) as-hydrolyzed cellulose nanocrystals.

The as-extracted cellulose from grape skins is shown as tens of micrometer scale, irregularly shaped cellulose solids by SEM (Fig. 5a). These cellulose pieces consist of bundles of cellulose microfibrils (Fig. 5b), attesting to the robust properties of grape cellulose following the rigorous organic/acid/base/oxidation isolation processes.

### 3.2. Preparation of nanostructures from grape cellulose

The as-extracted grape cellulose was further hydrolyzed by a typical sulfuric acid hydrolysis procedure (8.75 mL/g, 65% $H_2SO_4$, 45 °C, and 30 min) to prepare cellulose nanocrystals (CNCs). The chemical structure of cellulose was well retained after acid hydrolysis (Fig. 2c) while the CrI of the cellulose nanocrystals was increased to 64.3% from 54.9% of the as-extracted grape cellulose (Fig. 4b). Acid hydrolysis of wood, cotton and other sourced cellulose usually produces cellulose nanocrystals in the form of rods as widely reported in literature (Lucia, Habibi, & Rojas, 2010; Moon, Martini, Nairn, Simonsen, & Youngblood, 2011). Interestingly, TEM observation of grape cellulose nanocrystals showed only nano-scale spheres or nanoparticles (Fig. 6a). The diameters of these spherical cellulose nanoparticles ranged from 10 to 100 nm, with majority between 30 and 65 nm (Fig. 6b). Based on 169 TEM images of CNCs, these spherical cellulose nanoparticles have a calculated mean size of 48.1 (±14.6) nm.

The surface structure and morphology of these grape skin CNCs were further elucidated by AFM. The spherical nature of the as-hydrolyzed grape cellulose nanocrystals is clearly evident by both the phase and height images of AFM (Fig. 7). These grape cellulose spheres, however, appeared much larger with diameters ranging from 10 up to 350 nm, significantly larger than the 10–100 nm sizes observed by the TEM. All the heights of the cellulose spheres were well below 5 nm shown by the scale bar in Fig. 7a, or about one order of magnitude smaller than their diameters measured by AFM. Although AFM is known not to be accurate in determining lateral dimensions due to the tip broadening effect, the height image is by far highly accurate. In fact, the height or *z*-resolution calibrated for

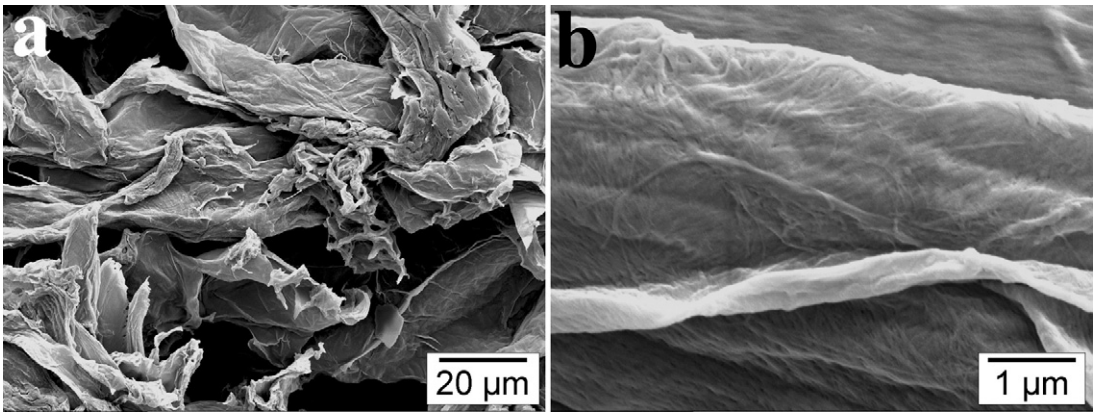


**Fig. 5.** SEM of (a) as-extracted cellulose and (b) the microfibrils isolated from grape skins.

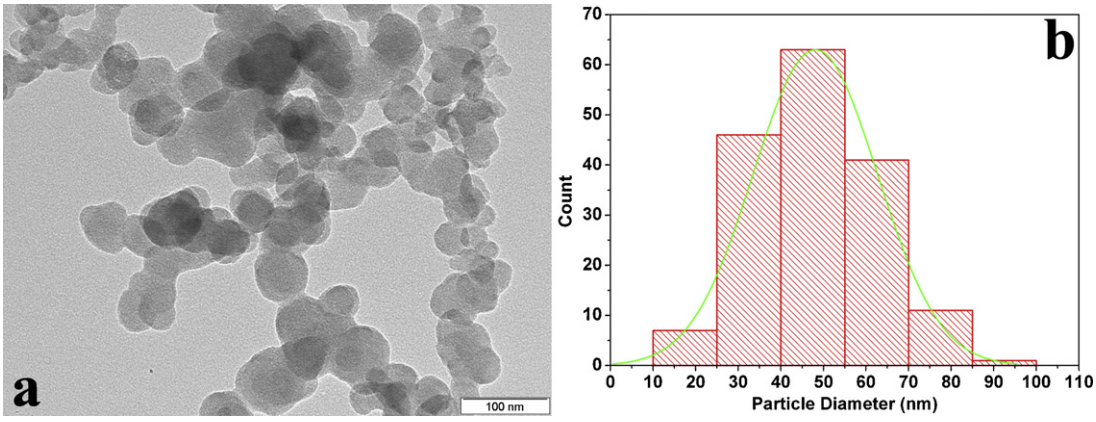


**Fig. 6.** Cellulose nanocrystals hydrolyzed from the grape skin cellulose: (a) TEM image and (b) size distribution (169 CNCs).

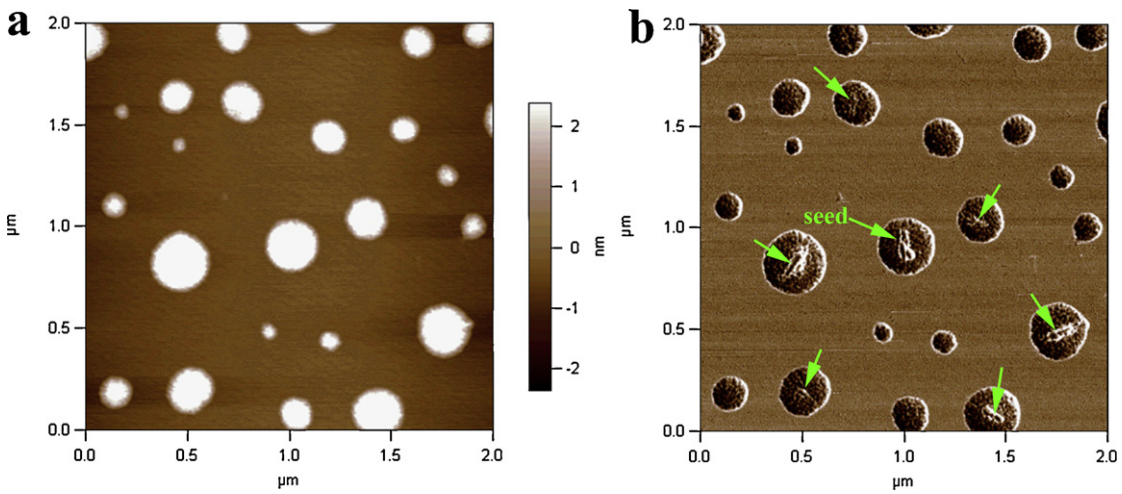


**Fig. 7.** AFM of grape skin cellulose nanocrystals: (a) height and (b) phase images.

this instrument is 0.06 nm. Therefore, the less than 5 nm height is highly accurate. The apparent far larger lateral dimensions by the AFM in comparison to those of TEM are intriguing. In addition to instrumental differences between these imaging techniques, the observed dimensional difference between AFM and TEM points to potential influence of the different surfaces, i.e., mica for AFM and carbon for TEM, upon which the same ultra-dilute (0.001, w/w%) aqueous CNC solutions were deposited and dried. One possible explanation is that the three-dimensional cellulose spheres remain intact with little or no deformation when deposited on the hydrophobic carbon surfaces of TEM grids whereas these cellulose spheres collapsed and flattened into thin circular disks upon drying

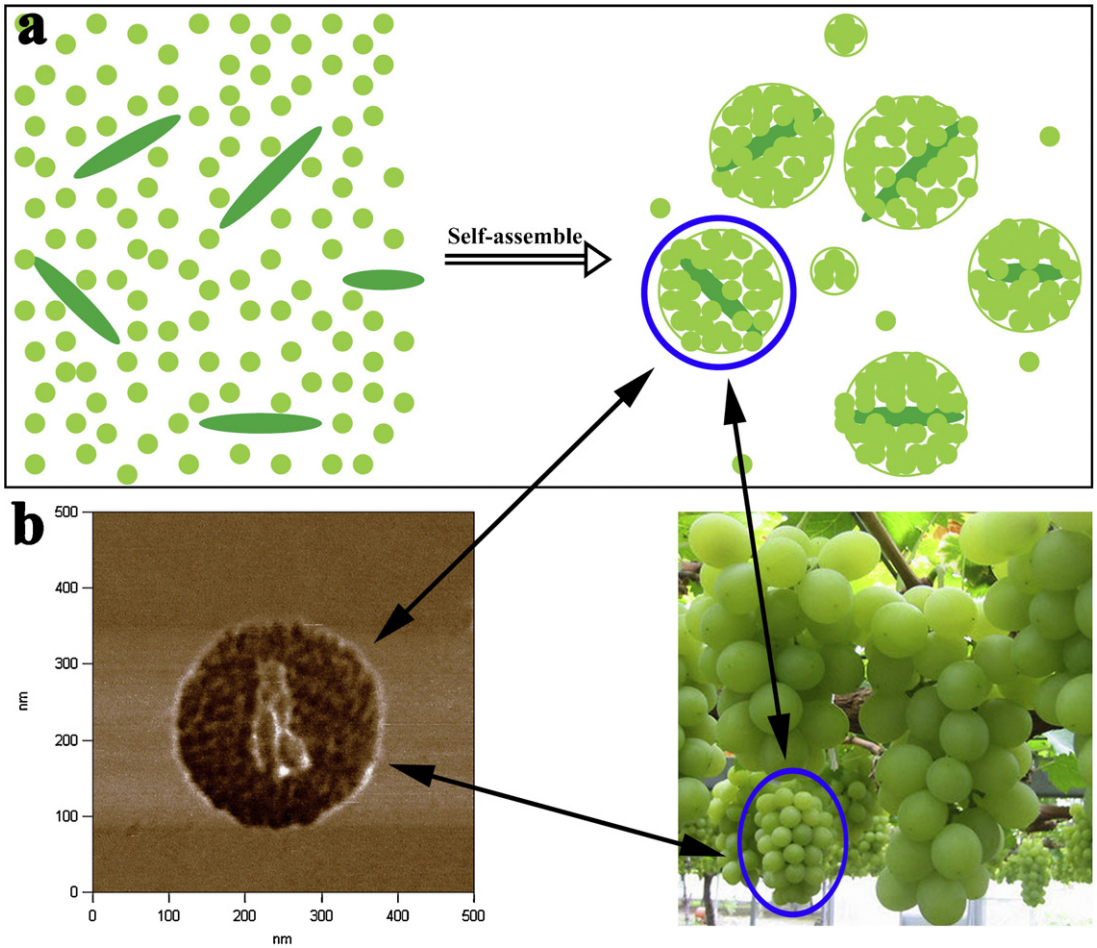


**Fig. 8.** (a) Schematic illustrating possible self-assembly of as-hydrolyzed grape cellulose nanocrystals and (b) AFM phase image of a nano-rod seeded cellulose core–shell spheres.

on the hydrophilic mica surface for the AFM. This raises the question on drying behaviors of cellulose nanostructure on different substrates that is being under further investigation. Most interestingly, the collapse of these cellulose spheres exposed unexpected detail of the interior structure as shown in the phase image (Fig. 7b). Most of these cellulose nanospheres, especially the larger ones, contained a nano-rod core surrounded by agglomerate of numerous tiny fragments. The nano-rods appeared in the AFM images to be at most 100–200 nm in lengths, overestimating due to the tip broadening effect, but should be less than 100 nm based on the more accurate measurements from TEM. The cellulose fragments were less than 5 nm, based on the highly accurate AFM height measurement. These imaging data suggest that grape skin CNCs were mainly nanoparticles that contained up to 20 nm long nano-rod seeded cores and numerous less than 5 nm diameter fragments as shells.

Although spherical cellulose nanoparticles have been produced by the hydrolysis of cellulose isolated from various biomass (Cheng, Wang, & Ding, 2008; Lu & Hsieh, 2010; Ragauskas, Zhang, Elder, & Pu, 2007), the exact structure and formation mechanism are largely unknown. It is commonly considered that cellulose in native plant cells is in the form of cellulose microfibrils and microfibrillar bundles that are imbedded amongst hemicellulose and lignin. Through chemical isolation and purification processes, cellulose in the forms of microfibrils and/or other fragmented forms is separated. During the collection and preparation processes, such as freeze-drying and deposition onto other substrates for imaging in our case, it is possible that the spherical cellulose nanoparticles were created by a self-assembly process from CNCs and their fragments.

Cellulose nanocrystals in rod-like shapes are usually produced from long chain, highly crystalline cellulose sources, such as cotton and wood, by acid hydrolysis of the less order domains leaving the large intact crystalline regions (Moon et al., 2011). The calculated CrI for the as-hydrolyzed grape CNCs is 64.3%, less crystalline than those from wood and cotton. In fact, CNCs from grape skins were mostly observed in the forms of nano-spheres and nano-fragments, to lesser degree, nano-rods, suggesting the grape skin cellulose to be less crystalline and less fibrillar. During drying, the more abundant nano-fragments associate around the fewer, but larger nano-rods by strong lateral hydrogen bonds and with each other, possibly driven by a layer-by-layer and thermodynamically favored process to the reduced specific surface. This possible self-assembly behavior depicted by the drawing shown in Fig. 8a is proposed for the observed core–shell cellulose nanostructure vividly shown in the AFM phase images (Fig. 8b). Interestingly, the core–shell cellulose nanoparticles are very similar to the shape of grape bundles, the starting biomass in this case.

## 4. Conclusions

Pure cellulose was successfully extracted from grape skins by an effective five-step process: organic extraction, acid and base treatments, and basic and acidic oxidation, to a total yield of 16.4%. The cellulose chemical structure was confirmed by FTIR, thermal analysis and XRD. Acid-hydrolysis of the as-extracted grape cellulose generated spherically shaped cellulose nanocrystals with diameters ranging from 10 to 100 nm and a 48.1 (±14.6) nm mean size as determined by TEM. AFM further disclosed that most of spherical nanoparticles actually consisted of 50 nm long nano-rods as cores surrounded by abundant cellulose nano-fragments less than 5 nm in sizes as the shells. It is highly possible that the core–shell cellulose nanostructure is created by the self-assembly process of cellulose fragments and rods induced from their strong interfacial hydrogen bonds.

## Acknowledgement

Provision of chardonnay grape skins by SonomaCeuticals is appreciated.

## References

Abe, K., & Yano, H. (2009). Comparison of the characteristics of cellulose microfibril aggregates of wood, rice straw and potato tuber. *Cellulose*, *16*(6), 1017–1023.
Alemdar, A., & Sain, M. (2008). Isolation and characterization of nanofibers from agricultural residues—Wheat straw and soy hulls. *Bioresource Technology*, *99*(6), 1664–1671.
Amendola, D., De Faveri, D. M., & Spigno, G. (2010). Grape marc phenolics: Extraction kinetics, quality and stability of extracts. *Journal of Food Engineering*, *97*(3), 384–392.
Brosse, N., Ping, L., Sannigrahi, P., & Ragauskas, A. (2011). Evaluation of grape stalks as a bioresource. *Industrial Crops and Products*, *33*(1), 200–204.
Cambardella, C. A., Richard, T. L., & Russell, A. (2003). Compost mineralization in soil as a function of composting process conditions. *European Journal of Soil Biology*, *39*(3), 117–127.
Cheng, R. S., Wang, N., & Ding, E. (2008). Preparation and liquid crystalline properties of spherical cellulose nanocrystals. *Langmuir*, *24*(1), 5–8.
Dong, S. P., & Roman, M. (2007). Fluorescently labeled cellulose nanocrystals for bioimaging applications. *Journal of the American Chemical Society*, *129*(45), 13810–13811.
FAOSTAT. (2009). *FAOSTAT Database: Food and Agriculture Organization of the United Nations*.
Gomez-Brandon, M., Lazcano, C., Lores, M., & Dominguez, J. (2011). Short-term stabilization of grape marc through earthworms. *Journal of Hazardous Materials*, *187*(1–3), 291–295.
Gomez-Plaza, E., Ortega-Regules, A., Romero-Cascales, I., Ros-Garcia, J. M., & Lopez-Roca, J. M. (2006). A first approach towards the relationship between grape skin cell-wall composition and anthocyanin extractability. *Analytica Chimica Acta*, *563*(1–2), 26–32.
Lorenzo, M., Moldes, D., Couto, S. R., & Sanroman, A. (2002). Improving laccase production by employing different lignocellulosic wastes in submerged cultures of Trametes versicolor. *Bioresource Technology*, *82*(2), 109–113.
Lu, P., & Hsieh, Y.-L. (2011). Preparation and characterization of cellulose nanocrystals from rice straw. *Carbohydrate Polymers*.
Lu, P., & Hsieh, Y. L. (2010). Preparation and properties of cellulose nanocrystals: Rods, spheres, and network. *Carbohydrate Polymers*, *82*(2), 329–336.
Lucia, L. A., Habibi, Y., & Rojas, O. J. (2010). Cellulose nanocrystals: Chemistry, self-assembly, and applications. *Chemical Reviews*, *110*(6), 3479–3500.
Meyer, A. S., & Arnous, A. (2008). Comparison of methods for compositional characterization of grape (*Vitis vinifera* L.) and apple (*Malus domestica*) skins. *Food and Bioproducts Processing*, *86*(C2), 79–86.
Meyer, A. S., Pinelo, M., & Arnous, A. (2006). Upgrading of grape skins: Significance of plant cell-wall structural components and extraction techniques for phenol release. *Trends in Food Science and Technology*, *17*(11), 579–590.
Moon, R. J., Martini, A., Nairn, J., Simonsen, J., & Youngblood, J. (2011). Cellulose nanomaterials review: Structure, properties and nanocomposites. *Chemical Society Reviews*, *40*(7), 3941–3994.
Nogi, M., Iwamoto, S., Nakagaito, A. N., & Yano, H. (2009). Optically transparent nanofiber paper. *Advanced Materials*, *21*(16), 1595–1598.
Nunan, K. J., Sims, I. M., Bacic, A., Robinson, S. P., & Fincher, G. B. (1997). Isolation and characterization of cell walls from the mesocarp of mature grape berries (*Vitis vinifera*). *Planta*, *203*(1), 93–100.
Paradelo, R., Moldes, A. B., & Barral, M. T. (2010). Utilization of a factorial design to study the composting of hydrolyzed grape marc and vinification lees. *Journal of Agricultural and Food Chemistry*, *58*(5), 3085–3092.
Pinelo, M., Rubilar, M., Jerez, M., Sineiro, J., & Nunez, M. J. (2005). Effect of solvent, temperature, and solvent-to-solid ratio on the total phenolic content and antiradical activity of extracts from different components of grape pomace. *Journal of Agricultural and Food Chemistry*, *53*(6), 2111–2117.
Ragauskas, A. J., Zhang, J. G., Elder, T. J., & Pu, Y. Q. (2007). Facile synthesis of spherical cellulose nanoparticles. *Carbohydrate Polymers*, *69*(3), 607–611.
Renneckar, S., & Li, Q. Q. (2011). Supramolecular structure characterization of molecularly thin cellulose. I. Nanoparticles. *Biomacromolecules*, *12*(3), 650–659.
Segal, L., Creely, J. J., Martin, A. E., & Conrad, C. M. (1959). An empirical method for estimating the degree of crystallinity of native cellulose using the X-ray diffractometer. *Textile Research Journal*, *29*(10), 786–794.
Souquet, J. M., Labarbe, B., Le Guerneve, C., Cheynier, V., & Moutounet, M. (2000). Phenolic composition of grape stems. *Journal of Agricultural and Food Chemistry*, *48*(4), 1076–1080.
Spigno, G., & De Faveri, D. M. (2007). Antioxidants from grape stalks and marc: Influence of extraction procedure on yield, purity and antioxidant power of the extracts. *Journal of Food Engineering*, *78*(3), 793–801.
Spigno, G., Pizzorno, T., & De Faveri, D. M. (2008). Cellulose and hemicelluloses recovery from grape stalks. *Bioresource Technology*, *99*(10), 4329–4337.
Sun, J. X., Sun, X. F., Zhao, H., & Sun, R. C. (2004). Isolation and characterization of cellulose from sugarcane bagasse. *Polymer Degradation and Stability*, *84*(2), 331–339.

Sun, R. C., Tomkinson, J., Mao, F. C., & Sun, X. F. (2001). Physicochemical characterization of lignins from rice straw by hydrogen peroxide treatment. *Journal of Applied Polymer Science*, *79*(4), 719–732.

Vazquez, M., Moldes, A. B., Dominguez, J. M., Diaz-Fierros, F., & Barral, M. T. (2007). Evaluation of mesophilic biodegraded grape marc as soil fertilizer. *Applied Biochemistry and Biotechnology*, *141*(1), 27–36.

Vazquez, M., Moldes, A. B., Dominguez, J. M., Diaz-Fierros, F., & Barral, M. T. (2008). Negative effect of discharging vinification lees on soils. *Bioresource Technology*, *99*(13), 5991–5996.

Wada, M., Heux, L., & Sugiyama, J. (2004). Polymorphism of cellulose I family: Reinvestigation of cellulose IV. *Biomacromolecules*, *5*(4), 1385–1391.